JOURNAL OF THERMOPHYSICS AND HEAT TRANSFER
Vol. 15, No. 2, April–June 2001

Natural Convection in a Trapezoidal Enclosure with Offset Baffles

F. Moukalled*
American University of Beirut, Beirut, Lebanon
and
S. Acharya†
Louisiana State University, Baton Rouge, Louisiana, 70803

A numerical investigation has been made of natural convection heat transfer in a trapezoidal enclosure (representing attic spaces) with offset baffles. Two thermal boundary conditions representing summerlike conditions (upper surface heated) and winterlike conditions (upper surface cooled) and two baffle heights are studied. For each boundary condition and baffle height, two baffle positions are considered. In position I, the upper baffle is offset toward the heated vertical wall and the lower baffle is offset toward the symmetry plane of the enclosure, whereas in position II, the upper baffle is offset toward the symmetry plane and the lower baffle is offset toward the heated wall. Rayleigh number values range from 10^3 to 5×10^7 for summerlike conditions and from 10^3 to 10^6 for winterlike conditions. Predictions reveal a decrease in heat transfer in the presence of baffles. In winterlike conditions, convection starts to dominate at a Rayleigh number much lower than that in summerlike conditions. The maximum reduction in heat transfer is achieved with long baffles placed in position II for summerlike conditions and in position I for winterlike conditions. Average Nusselt number correlation for both boundary conditions are presented.

Nomenclature

BH	=	baffle height
BL	=	baffle location
H	=	height of the short vertical wall
k	=	thermal conductivity
k_b	=	baffle thermal conductivity
k_r	=	conductivity ratio, k_b/k
Nu, Nu^*	=	local and normalized local Nusselt number
$\overline{Nu}$, $\overline{Nu}^*$	=	average and normalized average Nusselt number
Nu_0	=	local Nusselt number for pure conduction, $Ra = 0$
p, P	=	dimensional and dimensionless pressure
S	=	distance along wall
T	=	dimensional temperature
u, U	=	dimensional and dimensionless horizontal velocity component
v, V	=	dimensional and dimensionless vertical velocity component
W	=	half-width of the cavity
x, X	=	dimensional and dimensionless coordinate along the horizontal direction
y, Y	=	dimensional and dimensionless coordinate along the vertical direction

Subscripts

c, h	=	cold and hot wall
d, u	=	lower and upper wall
max	=	maximum value

Introduction

SEVERAL studies dealing with natural convection in undivided trapezoidal enclosures have been reported. Iyican et al.[1,2] presented experimental and numerical results for natural convection in an inclined trapezoidal cavity formed by parallel cylindrical cold top and hot bottom walls and plane adiabatic sidewalls. Similar experimental and numerical results were reported by Lam et al.[3] for a trapezoidal cavity composed of two vertical adiabatic sidewalls, a horizontal heated bottom wall, and an inclined cold top wall. Their work revealed that, under the boundary conditions used, a two-dimensional numerical model is sufficient to predict heat transfer rates to an acceptable level of accuracy, but it cannot describe the three-dimensional flowfield that occurs in the cavity. Karyakin[4] investigated transient natural convection in a trapezoidal cavity with parallel top and bottom walls and inclined sidewalls. Lee[5] and Peric[6] presented numerical results, up to a Rayleigh number of 10^5, for laminar natural convection in trapezoidal enclosures with horizontal bottom and top walls that are insulated and inclined sidewalls that are maintained at different uniform temperatures. Computations in the same geometry were carried out by Sadat and Salagnac[7] using a control-volume-based finite element technique for values of Rayleigh number ranging from 10^3 to 2×10^5. Further results in the same geometry were reported by Kuyper and Hoogendoorn[8] for Rayleigh numbers between 10^4 and 10^8.

Several investigations[9–11] dealing with natural convection heat transfer in a triangular enclosure have also been reported. This configuration may be viewed as a special case of a trapezoidal cavity whose lower and upper surfaces are not parallel. The work of Poulikakos and Bejan[9,10] revealed that, even at the highest value of Rayleigh number considered, when cooling the top inclined wall of the enclosure, the natural circulation within the cavity is composed of a single cell. Salmun[11] solved numerically the same problem and showed that the general flow structure corresponds to a single convective cell for low values of Rayleigh number and to multiple convective cells for high values of this parameter.

The interest in natural convection in triangular and trapezoidal enclosure stems from their applications in energy conservation in buildings and attic spaces, as well as in other applications such as solar collectors, cabin spaces, and so on. However, all of the preceding referenced studies have dealt with nonpartitioned enclosures. In some applications, such as energy conservation in a building or attic space, it may be advantageous to introduce partial dividers to reduce heat transfer. Furthermore, in office or industrial workplaces, office dividers and other partitions are commonly employed, and the effect of these partitions on the heat transfer in the enclosure is of interest.

Received 19 November 1999; revision received 19 September 2000; accepted for publication 21 September 2000.

*Professor, Department of Mechanical Engineering.
†Professor, Mechanical Engineering Department. Member AIAA.

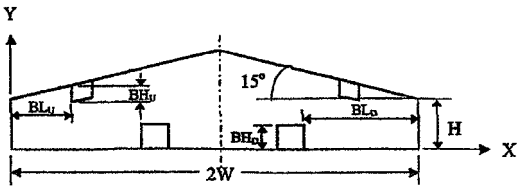

Fig. 1 Schematic of the physical domain.

Work on buoyancy-induced heat transfer in partially divided trapezoidal cavities has been limited to the studies reported in Refs. 12 and 13. In their work, Moukalled and Acharya[12,13] dealt with natural convection heat transfer in a partially divided trapezoidal cavity with the partial divider being attached to the lower horizontal base[12] or the upper inclined plane[13] of the cavity. For both bottom-heated and bottom-cooled boundary conditions used, results presented show that the presence of a baffle decreases heat transfer. In neither of these two reported studies were the effects of offset baffles on the flow and heat transfer behavior been considered. It is the intent of this paper to investigate buoyancy-induced heat transfer in a trapezoidal enclosure with two offset partial vertical dividers attached to the upper inclined plane and the lower horizontal base of the cavity. The novel contributions of the paper are to identify the effect of baffle positions on the heat transfer in a trapezoidal enclosure. It is important to understand these effects to design building spaces efficiently. The effect of baffle positions have not been previously reported in the literature and represents the primary focus of the present paper.

Physical Model and Assumptions

The physical situation under consideration, representing an attic space or an industrial building, is schematically shown in Fig. 1. Solutions for natural convection within the cavity, with air as the working fluid, are obtained for two different boundary conditions. In the first, the bottom wall of the cavity is maintained at the uniform cold temperature T_c, and all other walls are maintained at the uniform hot temperature T_h. In the second, the bottom wall is hot, T_h, while the temperature of all other walls is T_c. If the cavity represents an attic space, for example, then the first boundary condition resembles conditions in the attic during a summer day, with the vertical and top walls exposed to the hot ambient and the lower surface exposed to the air-conditioned interior at a lower temperature. Likewise, the second boundary condition simulates wintertime conditions in the attic with the vertical and top walls exposed to the cold ambient and the lower surface adjoining the heated interior of the building. In both cases, the effects of symmetrically mounting two pairs of offset baffles or partial dividers to the upper inclined and lower horizontal planes of the cavity (Fig. 1), on the heat transferred to or from an adjacent space are studied. Because of symmetry around the y axis, computations are performed in only half of the physical domain.

In the configuration studied, the half-width of the cavity, W, is four times the height H of the short vertical wall. The inclination of the top wall of the cavity is fixed at 15 deg. Two baffle heights for the upper baffle, BH_u, and the lower baffle, BH_d, equal to one-third and two-thirds the height of the cavity at the baffle location are considered. Also, two baffle positions, $\mathrm{BL}_u = W/3$, $\mathrm{BL}_d = 2W/3$ (position I) and $\mathrm{BL}_u = 2W/3$, $\mathrm{BL}_d = W/3$ (position II), are investigated. In all computations, the baffle thickness (BT) is taken as $\mathrm{BT} = W/20$, to simulate a thin baffle.

The equations governing the flow and heat transfer are those expressing the conservation of mass, momentum, and energy. The flow is assumed to be laminar, steady, and two dimensional with constant fluid properties, except for the induced variations in the body force term. In the baffle region, the only conservation equation needed is the Laplace equation for heat conduction. In addition, the energy balance at the baffle–air interface and the boundary conditions along the enclosure walls have to be satisfied.

Solution Procedure

The collocated control-volume-based numerical procedure of Rhie and Chow[14] that embodies the SIMPLE algorithm of Patankar[15] is employed to arrive at the solution to the coupled system of equations governing the flow and temperature fields. The calculations are performed on a curvilinear grid that is generated using the transfinite interpolation technique.[16] In generating the grid, control volume faces are arranged to lie along the baffle–air interfaces. The presence of the dividers in the calculation domain is accounted for by the special approach suggested by Patankar.[15] With this approach, the baffle region is treated as an infinitely viscous fluid (numerically specified as a very large value) with a nondimensional thermal conductivity corresponding to that of the baffle. This procedure leads to essentially zero velocities in the baffle region, and the energy equation reduces to that of the Laplace heat conduction equation. Because a conservative scheme is used, arranging the control volume faces to coincide with the divider interface ensures energy balance at the baffle–air interface.

Numerical Accuracy

All calculations have been done on a 120×120 nonuniform grid with the grid points clustered more closely along all solid boundaries where large gradients are expected. The choice of the grid point distribution was based on a number of preliminary calculations with successively finer grids. The accuracy of the calculations was verified by comparing representative computed profiles of velocity, temperature, and local Nusselt number using a 120×120 nonuniform grid with those obtained on a 160×160 grid. The maximum difference between the two solutions in the various quantities predicted was smaller than 0.69%. Conservation for the various physical quantities was satisfied to within 0.001% in each control volume. Results obtained were also compared with those generated using the well-known FLOW-3D commercial computational fluid dynamics code. The difference in the average Nusselt numbers for the cases studied was found to be less than 0.05%. As a further check for accuracy, computations were performed for a nonpartitioned trapezoidal enclosure using the boundary conditions of Lam et al.[3] Excellent agreement with their heat transfer results was found.

Results and Discussion

The governing parameters in the problem are the Prandtl number Pr, the Rayleigh number Ra, the conductivity ratio k_r, the heights of the upper and lower baffles BH_u and BH_d, and the relative position of the offset baffles, positions I and II. Air is considered to be the working fluid and the Prandtl number is assigned the value of 0.72. The conductivity ratio is fixed at 2 to simulate a poorly conducting divider. As noted earlier, results are obtained for two baffle heights, $\mathrm{BH}_u = H_u/3$ and $2H_u/3$ and $\mathrm{BH}_d = H_d/3$ and $2H_d/3$ (for notational convenience, $\mathrm{BH}_u = H_u/3$ and $\mathrm{BH}_d = H_d/3$ are denoted by $\mathrm{BH}_{u,d} = H_{u,d}/3$); two offset baffle configurations, $\mathrm{BL}_u = W/3$ and $\mathrm{BL}_d = 2W/3$ (position I) and $\mathrm{BL}_u = 2W/3$ and $\mathrm{BL}_d = W/3$ (position II); and Rayleigh number values varying between 10^3 and 5×10^7 for summertime conditions and between 10^3 and 10^6 for wintertime conditions.

For summertime conditions, results are presented in the form of representative streamlines and isotherms, midwidth horizontal velocity and temperature profiles, and local and average Nusselt number values. For wintertime conditions, only average heat transfer results are presented. This is because a two-dimensional model cannot adequately describe the three-dimensional flowfield that occurs in the cavity; however, it can predict, as revealed by the work of Lam et al.,[3] heat transfer rates to an acceptable level of accuracy.

Summertime Boundary Conditions

Streamlines and Isotherms

Streamline and isotherm plots are displayed in Figs. 2–5. The maximum stream function values $|\psi_{\max}|$ shown in Figs. 2–5 indicate that the strength of the flow increases with Rayleigh number. Moreover, at constant Rayleigh number values and for both offset baffle positions, it generally decreases with increasing baffle height.

For position I, the flow patterns and temperature distributions are shown in Figs. 2 and 3 for $\mathrm{BH}_{u,d} = H_{u,d}/3$ and $2H_{u,d}/3$, respectively. Results for the shorter baffle configuration (Fig. 2) indicate

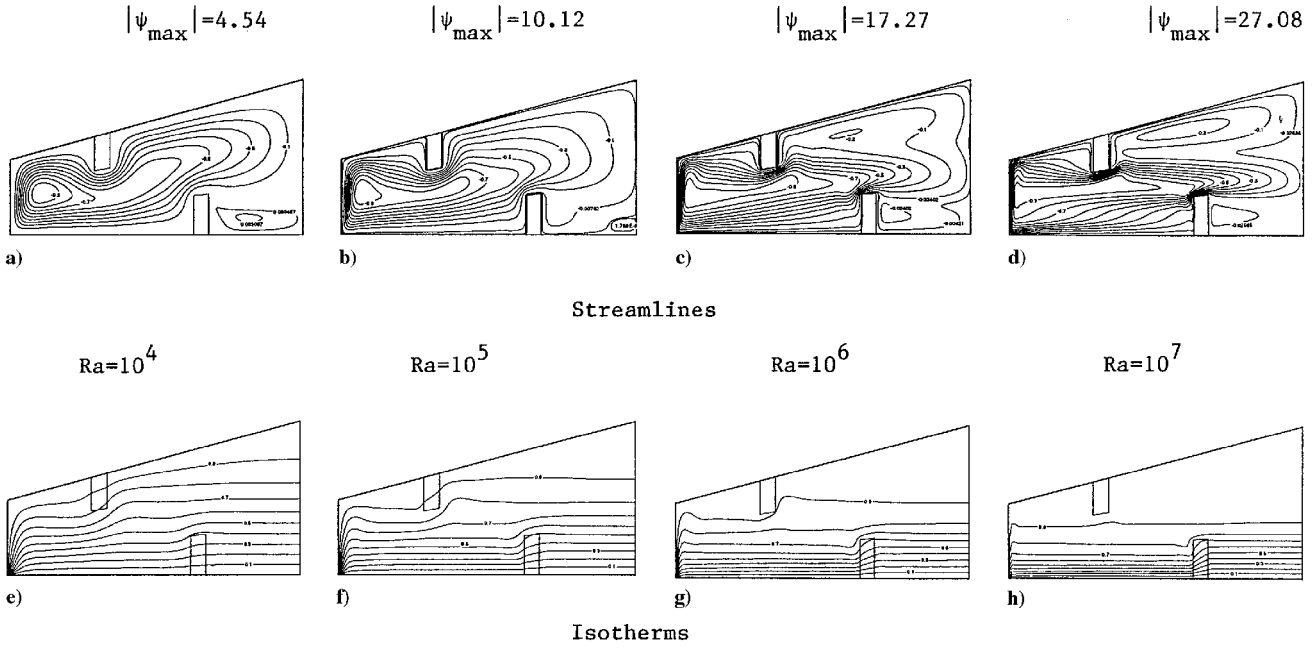

Fig. 2 Streamline and isotherm plots for $BH_{u,d} = H_{u,d}/3$, position I, summer.

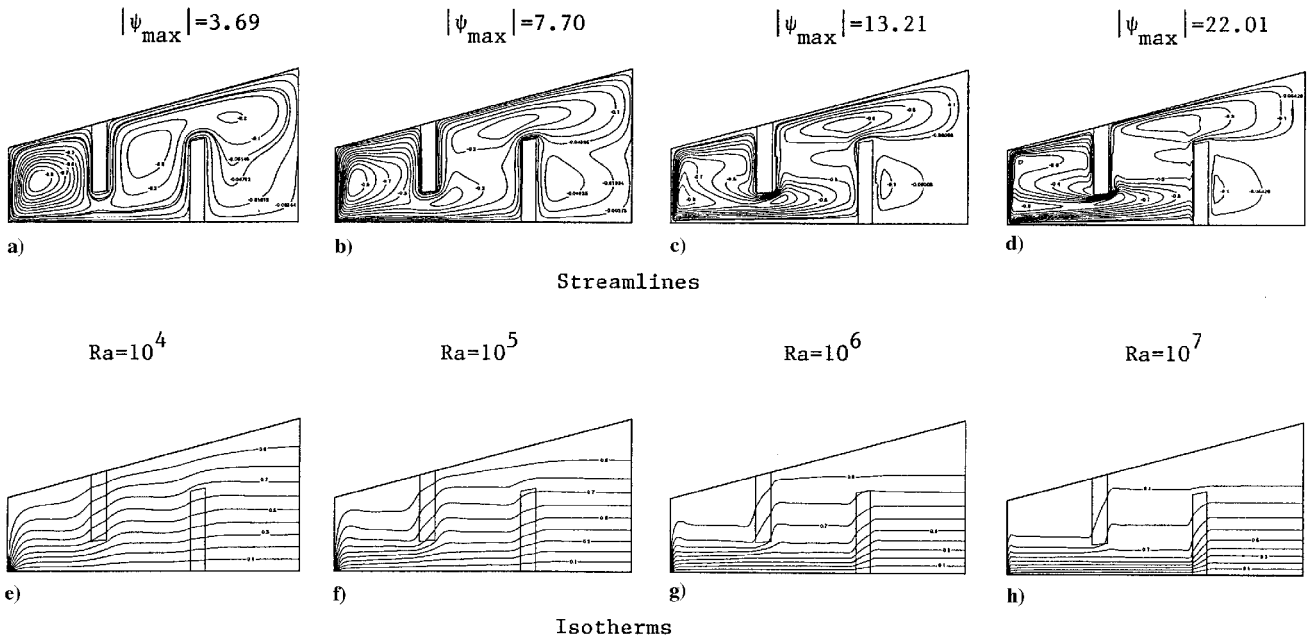

Fig. 3 Streamline and isotherm plots for $BH_{u,d} = 2H_{u,d}/3$, position I, summer.

that at $Ra = 10^4$ (Fig. 2a) the flow consists of a clockwise rotating eddy in addition to a small recirculation bubble to the right of the lower vertical divider. The clockwise rotation of the flow indicates that it moves up along the hot vertical and inclined walls, negotiates around the upper baffle, moves down along the symmetry line, and then detaches from the symmetry line toward the tip of the lower baffle. This detachment is due to the inability of the flow moving down the symmetry line to penetrate into the lower right portion of the enclosure. The detachment, therefore, leads to the formation of a separate counterclockwise eddy between the lower baffle and the symmetry plane. The eye of the main clockwise eddy is close to the vertical hot wall of the enclosure, where the largest velocities are located. As Rayleigh number increases (Figs. 2b–2d), the eye elongates and moves even closer to the hot vertical wall. In addition, due to increased thermal stratification at the higher Rayleigh numbers (Figs. 2g and 2h), it becomes more difficult for the flow to penetrate into the upper right portion of the domain, and therefore, the flow strength in the upper regions of the enclosure is considerably reduced. In Fig. 2, this manifests itself as a fast moving eddy in the lower portion of the enclosure and a slow moving recirculation in the stratified upper right corner

For the longer baffle configuration (position I, Fig. 3), results indicate that at the lowest Rayleigh number presented, $Ra = 10^4$, the recirculating flow exhibits three vortex cores within one overall rotating eddy (Fig. 3a). These three inner vortices rotate in the clockwise direction. As Rayleigh number increases, $Ra = 10^5$, a fourth vortex is formed in the lower right portion of the domain, and the vortices move to the left (Fig. 3b). Further increase in Rayleigh number, $Ra = 10^6$ and 10^7 (Figs. 3c and 3d) results in separation of the fourth vortex and further movement of the original vortices to the left. This is due to the higher stratification level in the upper right portion of the domain. Moreover, the strongest vortex is located close to the hot vertical wall, which, on leaving the lower tip of the upper baffle, forms a jetlike flow that impinges on the

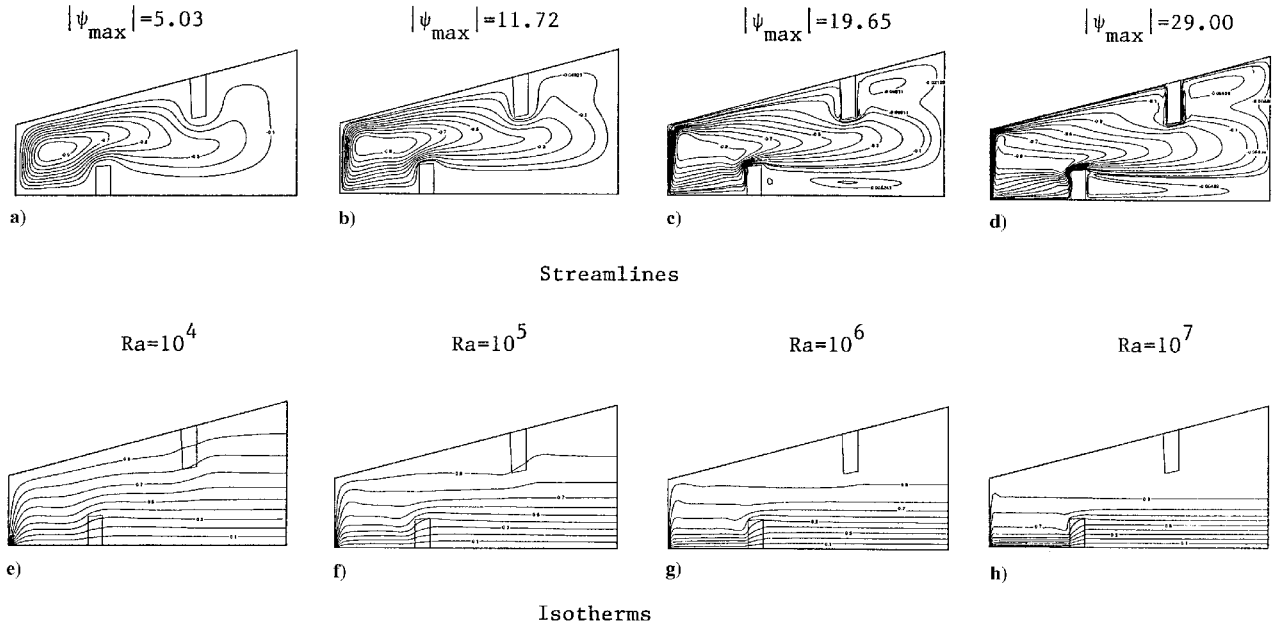

Fig. 4 Streamline and isotherm plots for $BH_{u,d} = H_{u,d}/3$, position II, summer.

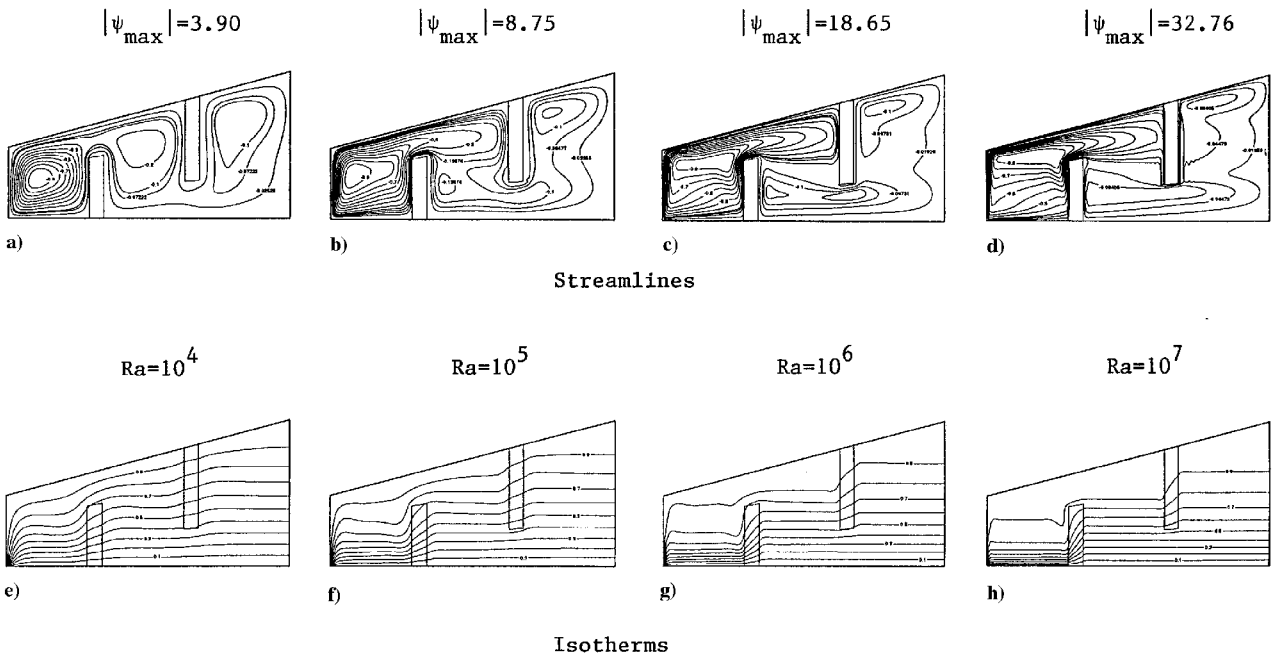

Fig. 5 Streamline and isotherm plots for $BH_{u,d} = 2H_{u,d}/3$ position II, summer.

lower baffle. Flow detachment along the symmetry line also leads to a jetlike flow in the upper right portion of the domain. Isotherms presented in Figs. 3e–3h reveal the same behavior as in Figs. 2e–2h. When isotherms in Figs. 2 and 3 are compared, it is obvious that longer baffles result in less packed isotherms, indicating lower heat transfer rates.

For position II, streamline and isotherm maps are shown in Figs. 4 and 5 for $BH_{u,d} = H_{u,d}/3$ and $2H_{u,d}/3$, respectively. For this configuration, the maximum strength of the flow, at a given value of Rayleigh number, is higher than the corresponding value obtained for position I. This is because the flow has a longer distance to travel along the heated wall before encountering the upper baffle. In other words, the interruption of the natural convection stream rising along the hot wall is delayed for position II, and consequently, higher natural convection velocities are achieved.

For $BH_{u,d} = H_{u,d}/3$ (Fig. 4), the general feature of the flow at Rayleigh number values of 10^4 and 10^5 (Figs. 4a and 4b) is composed of a clockwise-rotating eddy. At higher values (Figs. 4c and 4d), the flows to the right of the lower and upper baffles separate creating regions of low heat transfer rates. The effect of Rayleigh number on isotherms (Figs. 4e–4h) is similar to those presented earlier. However, the way baffles are positioned causes a denser clustering of isotherms to occur over a shorter distance to the left of the lower baffle. As will be shown later, this will lead to lower heat transfer levels, as compared to position I.

For the longer baffles (Fig. 5), stratification in the upper regions is weaker relative to that observed for the shorter baffles. As the Rayleigh number is increased, flow separates as a jet stream from the right baffle toward the tip of the left baffle. However, separation from the symmetry line is not observed for this case, and instead, at $Ra = 10^6$ and 10^7, a relatively weak jet that separates from the left baffle toward the tip of the right baffle is observed. These two separated jet streams lead to two recirculating eddies at the higher Rayleigh numbers, as seen in Figs. 5c and 5d.

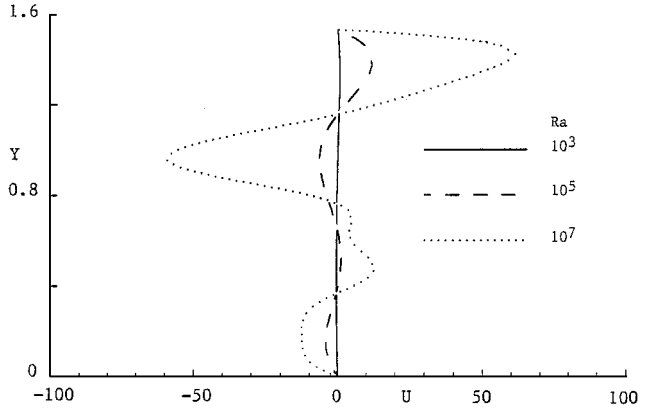

a) Velocity

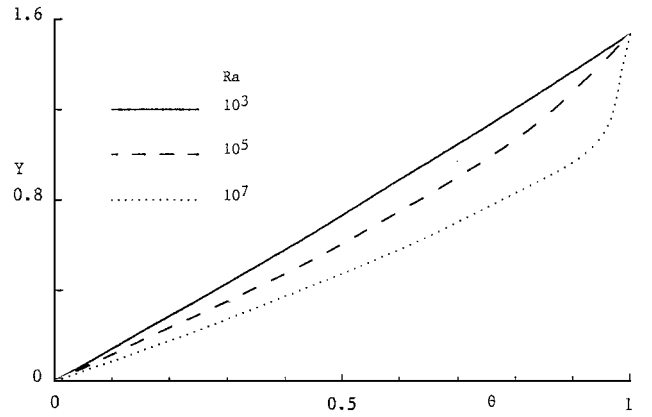

b) Temperature

Fig. 6 Profiles at $X = W/2H$ for $BH_{u,d} = 2H_{u,d}/3$, position II, summer.

Velocity and Temperature Profiles

Figures 6a and 6b show, respectively, the horizontal velocity and temperature distributions at $X = W/2H$ for an enclosure with offset baffles in position II. The velocity profiles (Fig. 6a) reflect the flow-fields presented in Figs. 5b and 5d. At $Ra = 10^3$, the flow is weak (velocity very close to zero) indicating a conduction-dominant heat transfer mode. The flow strength increases with increasing Rayleigh number values with boundary-layer behavior evident along the heated inclined wall. In the midregions, $0.4 < Y < 1.2$, the negative velocities associated with flow detachment toward the left baffle, and the positive velocities associated with flow detachment toward the right baffle can be observed. It is evident that the flow detachment in the upper half of the enclosure is nearly five times as strong as the detachment along the lower half.

At low Rayleigh number values, the variation in temperature (Fig. 6b) across the cavity at $X = W/2H$ is almost linear, reflecting the uniform distribution of isotherms shown in Fig. 5. At higher Rayleigh number values, this linear variation is retained over a portion of the enclosure that decreases in height as Rayleigh number increases, that is the temperature varies linearly up to a critical height $Y_c \cong 0.5$ and 0.25 at $Ra = 10^5$ and 10^7, respectively. Beyond that critical height, the rate of change in temperature starts to decrease until it reaches a very low value in the fully stratified upper portion of the cavity.

Nusselt Numbers

The local and average Nusselt numbers along the hot and cold walls are computed using the following definitions:

$$Nu_h = -\left.\frac{\partial T}{\partial n}\right|_h \Big/ (T_h - T_c)$$

$$Nu_c = -\left.\frac{\partial T}{\partial n}\right|_c \Big/ (T_h - T_c) \qquad (1)$$

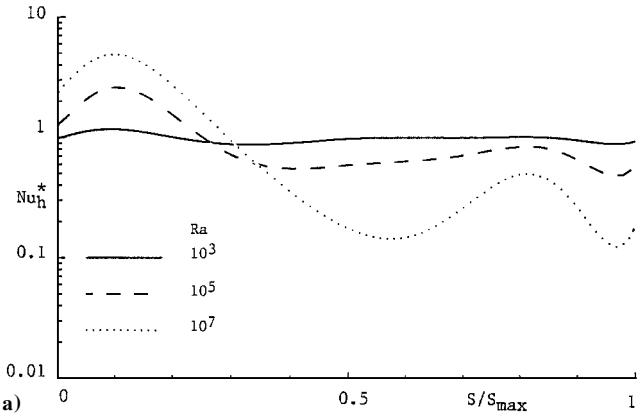

a)

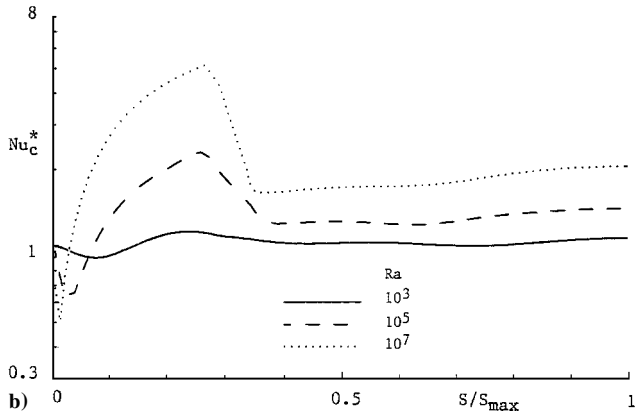

b)

Fig. 7 Local normalized Nusselt number distribution of the cavity for $BH_{u,d} = 2H_{u,d}/3$, position II, summer, along a) hot wall and b) cold wall.

$$\overline{Nu_h} = \frac{1}{S_{h,\max}} \int_0^{S_{h,\max}} Nu_h \, ds, \qquad \overline{Nu_c} = \frac{1}{S_{c,\max}} \int_0^{S_{c,\max}} Nu_c \, ds \qquad (2)$$

where n is the normal distance from the wall; S is the distance along the heated or cooled wall measured from its lowest point, $X = 0$, $Y = 0$; and $S_{h,\max}$ and $S_{c,\max}$ are the maximum possible lengths of the hot and cold walls, respectively. Since $\overline{Nu_h} = \overline{Nu_c}$, the subscript will be dropped and the average heat transfer will be denoted by Nusselt number $\overline{Nu}$. Moreover, to assess directly the relative effect of convection, the local and average Nusselt numbers are presented in the following normalized forms:

$$Nu^* = Nu/Nu_0, \qquad \overline{Nu^*} = \overline{Nu}/\overline{Nu_0} \qquad (3)$$

where Nusselt numbers Nu_0 and $\overline{Nu_0}$ are the local and average Nusselt number values for pure conduction, that is, at $Ra = 0$. The variations of Nusselt number Nu^* along the hot and cold walls are presented in Fig. 7a and 7b, respectively, for offset baffles in position II and of heights $2H_u/3$ and $2H_d/3$. Values are plotted as a function of $S/S_{\max}$, where $S_{\max}$ is the maximum possible value of S along the wall.

At low Rayleigh number values, $Ra = 10^3$, Nusselt number Nu_h^* distribution (Fig. 7a) indicates that conduction is the dominant heat transfer mode in the whole enclosure, $Nu_h^* \approx 1$. At high Rayleigh numbers and along the vertical portion of the hot wall, that is, $S_h/S_{h,\max} < 0.1945$, convection is the dominant heat transfer mode ($Nu_h^* > 1$) and Nusselt number Nu_h^* increases with increasing Rayleigh number values. The opposite is true along the inclined portion of the hot wall, $0.1945 < S_h/S_{h,\max} < 1$, where $Nu_h^* < 1$ over most of its length. This is caused by the strong stratification effects in the upper region as revealed by the isotherms shown in Fig. 5. Moreover, heat transfer along the inclined portion of the hot wall to the left of the divider, $0.1945 < S_h/S_{h,\max} < 0.7213$, passes by a minimum at a location $S_h/S_{h,\max} \cong 0.57$ midway between the lower and upper baffles, where stratification effects maximize. This minimum

Table 1 Average Nusselt number values

Ra	$BH_{u,d}=0$, no baffles	$BH_{u,d}=H_{u,d}/3$, position I	$BH_{u,d}=2H_{u,d}/3$, position I	$BH_{u,d}=H_{u,d}/3$, position II	$BH_{u,d}=2H_{u,d}/3$, position II
			Absolute conduction values, $\overline{Nu_0}$		
0	5.49204	5.567	5.66	5.5727	5.6668
			$\overline{Nu^*}$ *for summertime boundary conditions*		
10^3	1.010	1.0058	1.0049	1.0053	1.0053
10^4	1.107	1.076	1.055	1.069	1.056
10^5	1.307	1.273	1.182	1.244	1.177
10^6	1.659	1.602	1.5046	1.536	1.42
10^7	2.191	2.096	1.991	1.945	1.777
5×10^7	2.519	2.426	2.279	2.222	1.94
			$\overline{Nu^*}$ *for wintertime boundary conditions*		
10^3	1.185	1.011	1.0108	1.021	1.0193
10^4	2.317	1.688	1.578	1.7945	1.639
10^5	4.055	2.859	2.371	2.447	2.767
10^6	6.360	4.602	4.096	4.83	4.203

decreases with increasing Rayleigh number due to higher thermal stratification. To the right of the upper baffle, a peak is observed due to impingement of the flow negotiating around the upper baffle. The value of this peak decreases with increasing Rayleigh number due to more pronounced thermal stratification.

The Nusselt number distributions along the horizontal cold wall are shown in Fig. 7b. As expected, the level of Nusselt number increases with increasing Rayleigh number values. Moving from right to left along the the cold wall leads to a decrease in the values of the Nusselt number because the fluid is heated as it moves over the lower hot surface. Furthermore, due to the larger temperature gradients in the baffle at high Rayleigh number values (compare isotherms in Fig. 5e and 5h), a sharp increase in Nusselt number Nu_c^* in the baffle is obtained. Then, Nusselt number Nu_c^* decreases due to an increase in the temperature of the fluid carried by the separated jet that impinges first on the top of the left baffle, moves down along the baffle, and then to the left along the cold wall (Figs. 5c and 5d).

The normalized average Nusselt number values $\overline{Nu^*}$ and the average conduction values $\overline{Nu_0}$ for all cases studied are given in Table 1. Moreover, to assess and quantify the effects of baffles easily, results in a nonpartitioned trapezoidal cavity are also included.

At $Ra=10^3$, even though Nusselt number $\overline{Nu^*}$ is lower for the partitioned cavities as compared to the nonpartitioned cavity, Nusselt number $\overline{Nu}$ is higher, $\overline{Nu}=\overline{Nu^*}\times\overline{Nu_0}$. This is due to dominance of conduction at this low Rayleigh number and the higher value of the conduction heat transfer Nusselt number $\overline{Nu_0}$ in the partitioned enclosure caused by the higher conductivity of the baffles. The maximum increase in average Nusselt number is 2.70% and occurs with the longest baffles in offset position II. At moderate Rayleigh numbers, $Ra<10^5$, the overall heat transfer remains strongly dominated by conduction, that is, $\overline{Nu^*}<1.1$. However, due to the modest convection effects, the average Nusselt number values are lower in the partitioned cavities. The contribution of advection to the total heat transfer becomes as important as the conduction contribution at Rayleigh number between 10^6 and 10^7. Except for $Ra=10^3$, the presence of baffles decreases the overall heat transfer with the magnitude of decrease increasing with increasing BH. The reduction in the total heat transfer is greater in the offset baffle position II. Therefore, it is better to use this configuration to minimize heat gain in summer. Moreover, by comparing current estimates against results in partitioned cavities with a single baffle attached either to the lower base[12] or the upper inclined plane,[13] it is found that the maximum decrease in heat transfer for this offset configuration is close to the 19.25% reduction obtained in Ref. 12. Keeping in mind that at $Ra=10^3$ an increase in heat transfer is obtained, the use of offset baffles does not offer any advantage for summertime conditions over the configurations in Ref. 12.

The average Nusselt number values for summertime conditions, displayed in normalized form in Table 1, are correlated with a maximum deviation of less than ±13.10% via the following relation:

$$\overline{Nu}=2.94(Ra)^{0.08}\left(\frac{1+BL_u/W}{1+BL_d/W}\right)^{0.15}\left(\frac{1+BH_u/H}{1+BH_d/H}\right)^{0.05} \quad (4)$$

Wintertime Boundary Conditions

The local and average Nusselt numbers along the hot and cold walls are again computed using Eqs. (1) and (2), respectively. The effects on heat transfer of mounting offset baffles in positions I and II to the upper inclined plane and lower base of the cavity can be assessed by a direct comparison between the computed Nusselt number $\overline{Nu^*}$ values in nonpartitioned and partitioned enclosures presented in the lower part of Table 1.

Predicted values reveal that convection becomes important at relatively low Rayleigh number values. Thus, unlike the earlier observations for summertime conditions, reduction in heat transfer in the partitioned cavities is achieved at all Rayleigh number values including $Ra=10^3$. In general, for both offset baffle positions, the decrease in the overall heat transfer is greater with increasing height of the baffles. The highest decrease is obtained with the longest baffles, $BH_{u,d}=2H_{u,d}/3$, in offset position I. A comparison between current Nusselt number $\overline{Nu}$ estimates and those reported in Ref. 12 and 13 reveals that the maximum decrease in average Nusselt number for this configuration is about 39.74% compared to 31.51 and 34.00% for the configurations in Ref. 12 and 13, respectively. Therefore, for wintertime conditions, there is a slight advantage in using offset dividers with the upper one placed close to the hot vertical wall of the cavity. The average Nusselt number values for winterlike conditions, displayed in normalized form in Table 1, are correlated as

$$\overline{Nu}=1.33(Ra)^{0.21}\left(\frac{1+BL_u/W}{1+BL_d/W}\right)^{-0.32}\left(\frac{1+BH_u/H}{1+BH_d/H}\right)^{0.84} \quad (5)$$

with a maximum deviation of less than ±9.99%.

Conclusions

Natural convection in a trapezoidal cavity with offset baffles has been studied numerically. In particular, the effects of Rayleigh number, BH, and BL on heat transfer in summerlike (bottom-cooled) and winterlike (bottom-heated) conditions are investigated. For both boundary conditions, convection contribution to total heat transfer is found to increase with increasing Rayleigh number. Nevertheless, convection is by far more pronounced for wintertime conditions. The presence of baffles decreases heat transfer with a greater decrease observed at higher BH. For summerlike conditions, the highest reduction in heat transfer is obtained with tall baffles in offset position II (upper baffle offset toward the symmetry line). However, the use of offset baffles does not offer any additional advantage over the single-baffle configuration studied in Ref. 12. For winterlike conditions, the use of offset baffles is more advantageous than the

configurations in Refs. 12 and 13. The lowest heat transfer rate is accomplished with tall baffles in offset position I (upper baffle offset toward the heated wall).

Acknowledgments

The financial support provided by the University Research Board of the American University of Beirut through Grant 48720 is gratefully acknowledged. Computations were performed in the Department of Mechanical and Mechatronics Engineering at the University of Sydney, Sydney, Australia. Special thanks are due to M. Masri for allowing the use of his computational facilities and to D. Fletcher for performing the FLOW-3D computations.

References

[1]Iyican, L., Bayazitoglu, Y., and Witte, L., "An Analytical Study of Natural Convective Heat Transfer Within a Trapezoidal Enclosure," *Journal of Heat Transfer*, Vol. 102, No. 3, 1980, pp. 640–647.

[2]Iyican, L., Witte, L. C., and Bayazitoglu, Y., "An Experimental Study of Natural Convection in Trapezoidal Enclosures," *Journal of Heat Transfer*, Vol. 102, No. 3, 1980, pp. 648–653.

[3]Lam, S. W., Gani, R., and Simons, J. G., "Experimental and Numerical Studies of Natural Convection in Trapezoidal Cavities," *Journal of Heat Transfer*, Vol. 111, No. 2, 1989, pp. 372–377.

[4]Karyakin, Y. E., "Transient Natural Convection in Prismatic Enclosures of Arbitrary Cross-Section," *International Journal of Heat and Mass Transfer*, Vol. 32, No. 6, 1989, pp. 1095–1103.

[5]Lee, T. S., "Numerical Experiments with Fluid Convection in Tilted Nonrectangular Enclosures," *Numerical Heat Transfer*, Pt. A, Vol. 19, No. 5, 1991, pp. 487–499.

[6]Peric, M., "Natural Convection in Trapezoidal Cavities," *Numerical Heat Transfer*, Pt. A, Vol. 24, No. 2, 1993, pp. 213–219.

[7]Sadat, H., and Salagnac, P., "Further Results for Laminar Natural Convection in a Two-Dimensional Trapezoidal Enclosure," *Numerical Heat Transfer*, Pt. A, Vol. 27, No. 4, 1995, pp. 451–459.

[8]Kuyper, R. A., and Hoogendoorn, C. J., "Laminar Natural Convection Flow in Trapezoidal Enclosures," *Numerical Heat Transfer*, Pt. A, Vol. 28, No. 1, 1995, pp. 55–67.

[9]Poulikakos, D., and Bejan, A., "The Fluid Dynamics of an Attic Space," *Journal of Fluid Mechanics*, Vol. 131, 1983, pp. 251–269.

[10]Poulikakos, D., and Bejan, A., "Natural Convection in a Triangular Enclosure," *Journal of Heat Transfer*, Vol. 105, No. 3, 1983, pp. 652–655.

[11]Salmun, H., "Convection Patterns in a Triangular Domain," *International Journal of Heat and Mass Transfer*, Vol. 38, No. 2, 1995, pp. 351–362.

[12]Moukalled, F., and Acharya, S., "Buoyancy-Induced Heat Transfer in Partially Divided Trapezoidal Cavities," *Numerical Heat Transfer*, Pt. A, Vol. 32, No. 8, 1997, pp. 787–810.

[13]Moukalled, F., and Acharya, S., "Natural Convection in Trapezoidal Cavities with Baffles Mounted to Their Upper Inclined Planes," *Numerical Heat Transfer*, Pt. A, Vol. 37, No. 6, 2000, pp. 545–565.

[14]Rhie, C. M., and Chow, W. L., "Numerical Study of the Turbulent Flow Past an Airfoil with Trailing Edge Separation," *AIAA Journal*, Vol. 21, No. 11, 1983, pp. 1525–1532.

[15]Patankar, S. V., *Numerical Heat Transfer and Fluid Flow*, Hemisphere, New York, 1980.

[16]Gordon, W. J., and Theil, L. C., "Tranfinite Mappings and Their Applications to Grid Generation," *Numerical Grid Generation*, edited by J. F. Thompson, North–Holland, New York, 1982, pp. 171–192.